

Effects of Solid Solution Strengthening Elements Mo, Re, Ru, and W on Transition Temperatures in Nickel-Based Superalloys with High γ' -Volume Fraction: Comparison of Experiment and CALPHAD Calculations



NILS C. RITTER, ROMAN SOWA, JAN C. SCHAUER, DANIEL GRUBER, THOMAS GOEHLER, RALF RETTIG, ERWIN POVODEN-KARADENIZ, CAROLIN KOERNER, and ROBERT F. SINGER

We prepared 41 different superalloy compositions by an arc melting, casting, and heat treatment process. Alloy solid solution strengthening elements were added in graded amounts, and we measured the solidus, liquidus, and γ' -solvus temperatures of the samples by DSC. The γ' -phase fraction increased as the W, Mo, and Re contents were increased, and W showed the most pronounced effect. Ru decreased the γ' -phase fraction. Melting temperatures (*i.e.*, solidus and liquidus) were increased by addition of Re, W, and Ru (the effect increased in that order). Addition of Mo decreased the melting temperature. W was effective as a strengthening element because it acted as a solid solution strengthener and increased the fraction of fine γ' -precipitates, thus improving precipitation strengthening. Experimentally determined values were compared with calculated values based on the CALPHAD software tools Thermo-Calc (databases: TTNI8 and TCNI6) and MatCalc (database ME-NI). The ME-NI database, which was specially adapted to the present investigation, showed good agreement. TTNI8 also showed good results. The TCNI6 database is suitable for computational design of complex nickel-based superalloys. However, a large deviation remained between the experiment results and calculations based on this database. It also erroneously predicted γ' -phase separations and failed to describe the Ru-effect on transition temperatures.

<https://doi.org/10.1007/s11661-018-4730-0>
© The Author(s) 2018

I. INTRODUCTION

SINCE the introduction of nickel-based superalloys in industrial and aeronautical gas turbine applications, alloy development has mainly been performed on a “trial-and-error” basis. This experimental approach is expensive and time consuming with a relatively low

chance of success. In recent years, chemical optimization of nickel-based superalloys has often been supported by computational methods.^[1–4] These new numerical approaches are based on different mathematical search and optimization algorithms, which use semi-empirical and physical-based models to predict certain relevant properties. The development of alloys, such as STAL15,^[1] TMS-238,^[2] SGLS3,^[3] and ERBO/15^[4] for blade applications with the use of these new techniques has demonstrated their effectiveness for future alloy development.

One main physical property model used in such programs is the calculation of phase diagrams (CALPHAD) method. This method is based on minimizing the free energy of the investigated material at a certain temperature, composition, and pressure. Many detailed reports on the CALPHAD approach have been published.^[5–8] In principle the thermodynamic information regarding the structure and phase stability is stored in databases, which can be used in commercial software, such as Thermo-Calc, MatCalc, Pandat, FactSAGE,

NILS C. RITTER, JAN C. SCHAUER, DANIEL GRUBER, CAROLIN KOERNER, and ROBERT F. SINGER are with the Institute of Metals Science and Engineering, FAU Universität Erlangen, Erlangen, Germany. Contact e-mail: nils.ritter@fau.de ROMAN SOWA is with the MTU Aero Engines Polska, Rezeszow, Poland and also with the Institute of Nuclear Physics, Polish Academy of Sciences, Krakow, Poland. THOMAS GOEHLER is with the MTU Aero Engines AG, Munich, Germany. RALF RETTIG is with the Institute of Metals Science and Engineering, FAU Universität Erlangen and also with the ThermoCalc Software AB, Solna, Sweden. ERWIN POVODEN-KARADENIZ is with the Institute of Materials Science and Technology, TU Vienna, Vienna, Austria.

Manuscript submitted May 3, 2017.

Article published online June 12, 2018

and JMatPro. For example, with the aid of the CALPHAD application it is possible to calculate the phase composition and phase fraction dependence on alloy composition and temperature. This feature allows the user to design an alloy for specific demands if one is able to link the chemical composition and phase fraction to the mechanical properties.

The creep resistance of nickel-based superalloys is a basic feature in alloy development. Creep deformation at high temperatures and low stresses are controlled by thermally activated dislocation-motion in the γ -matrix phase (e.g., Reference 9). Furthermore, precipitation strengthening, provided by a high volume fraction of fine precipitates, and solid solution strengthening of the matrix phase are important. In particular, Mo, W, and especially Re^[10,11] are well known to increase the mechanical strength of the matrix phase and consequently the overall creep performance. The advantage of Ru is that in addition to solid solution strengthening, it also improves the phase stability, i.e., suppresses detrimental TCP (topological close-packed) phase formation; however, the exact mechanism of this effect remains unclear.^[12–16] In this paper, we compare the effects of the relevant elements.

We used the software packages Thermo-Calc with the databases TTNI8 and TCNI6 and the software MatCalc with the database ME-NI. We investigated the influence of the solid solution strengthening elements Mo, Re, Ru, and W on the transition temperatures and the phase occupation in terms of the γ -matrix and the γ' -precipitation phase. The database ME-NI was improved during the present investigation by optimizing the accuracy of the underlying binary and ternary base systems. These base systems are used for extrapolation of multicomponent nickel-based superalloys. We show that even small errors or deviations in the base systems

can have a pronounced effect on the results for a multicomponent alloy, especially in the presence of precipitation phases. Calculated values are compared with experimental results to determine the accuracy of existing databases.

II. METHODS

A. Alloy Chemistry and Processing

This study covers four groups of alloys. The first two groups were fabricated as polycrystalline alloys by arc melting with graded amounts of 1 and 2.5 at. pct Mo, Re, Ru, and W and without Ta (Group 1—EXP alloys without Ta). A group of Ta-containing materials (Group 2—EXP alloys with Ta) was also fabricated, as listed in Table I. The “as-solidified” microstructure was annealed in two steps: a homogenization heat treatment (10 K/min up to 1300 °C/1 hour, 1310 °C/1 hour, and 1320 °C/4 hours, cooling in ambient air) and an aging heat treatment (4 K/min up to 860 °C, 1 K/min up to 900 °C/30 hours, cooling in ambient air). Complete homogeneity of the elements was achieved in all group 1 and 2 alloys.

The third group referred to as “Astra alloys” (Table II) is based on the work of Heckl *et al.*^[17] In our earlier study, the Re and Ru contents were varied, starting from the base composition of CMSX-4. These directionally solidified alloys were heat treated as described in Reference 17. The fourth group (referred to as “ERBO alloys”) consisted of experimental nickel-based superalloys for blade applications, which were investigated at our institute in the framework of the Collaborative Research Center SFB TR 103. All elements could be completely homogenized, except for some residual segregation of Re in the dendritic core.

Table I. Polycrystalline Alloys with Various Contents of Solid Solution Strengtheners (Mo, Re, Ru, and W)

At. Pct	Al	Co	Cr	Mo	Re	Ru	Ta	W
Group 1: EXP alloy system without Ta								
EXP1	12.5	12.5	7.5					
EXP2	12.5	12.5	7.5	1.0				
EXP3	12.5	12.5	7.5	2.5				
EXP4	12.5	12.5	7.5		1.0			
EXP5	12.5	12.5	7.5		2.5			
EXP6	12.5	12.5	7.5			1.0		
EXP7	12.5	12.5	7.5			2.5		
EXP8	12.5	12.5	7.5					1.0
EXP9	12.5	12.5	7.5					2.5
Group 2: EXP alloy system with Ta								
EXP10	12.5	12.5	7.5				2.5	
EXP11	12.5	12.5	7.5	1.0			2.5	
EXP12	12.5	12.5	7.5	2.5			2.5	
EXP13	12.5	12.5	7.5		1.0		2.5	
EXP14	12.5	12.5	7.5		2.5		2.5	
EXP15	12.5	12.5	7.5			1.0	2.5	
EXP16	12.5	12.5	7.5			2.5	2.5	
EXP17	12.5	12.5	7.5				2.5	1.0
EXP18	12.5	12.5	7.5				2.5	2.5

Alloy group 1 with no Ta, alloy group 2 with Ta. Ta-containing alloys exhibited a higher γ' -phase fraction.

Table II. Directionally Solidified Alloys with Various Amounts of Re and Ru Together with ERBO/20 (Corresponding to EPM102)^[18] and ERBO/21 (Corresponding to TMS-238)^[2]

At. pct	Al	Co	Cr	Mo	Re	Ru	Ta	W
Group 3: Astra alloys								
Astra 00	13.50	9.00	6.00	0.60			2.20	2.00
Astra 02	13.50	9.00	6.00	0.60		2.00	2.20	2.00
Astra 10	13.50	9.00	6.00	0.60	1.00		2.20	2.00
Astra 11	13.50	9.00	6.00	0.60	1.00	1.00	2.20	2.00
Astra 12	13.50	9.00	6.00	0.60	1.00	2.00	2.20	2.00
Astra 14	13.50	9.00	6.00	0.60	1.00	4.00	2.20	2.00
Astra 20	13.50	9.00	6.00	0.60	2.00		2.20	2.00
Astra 21	13.50	9.00	6.00	0.60	2.00	1.00	2.20	2.00
Astra 22	13.50	9.00	6.00	0.60	2.00	2.00	2.20	2.00
Astra 23	13.50	9.00	6.00	0.60	2.00	3.00	2.20	2.00
Group 4: ERBO alloys (incomplete selection)								
ERBO20	13.27	18.97	2.38	1.35	2.06	1.92	2.94	2.11
ERBO21	13.84	6.98	5.60	0.73	2.18	3.13	2.66	1.38

From each of these 41 heat-treated alloys, cubes having dimensions of 3 mm were cut and used for differential scanning calorimetry (DSC) measurements on a Netzsch STA 409C/CD (Netzsch GmbH, Selb, Germany) apparatus. The heat-treated state was used instead of the as-cast state because otherwise the γ' -solvus temperature could not be determined clearly owing to peak broadening and microsegregation occurring during the solidification process. The solidus temperature is also strongly influenced by these effects (see Figure 1(a)). Additionally, the homogenized state is much closer to the equilibrium conditions (CALPHAD calculation) than the as-cast state. The DSC device was calibrated against the solidus temperature of pure elements (Ni, Co, and Cu) with an absolute error of less than 1 K. The transformation temperatures were determined by plotting the DSC-signal (W/mg) against temperature ($^{\circ}$ C) and tracking the deviation to the base line of the heating curve. The γ' -solvus was not clearly visible in the cooling curves and therefore, the heating curves are used. Also, the transition temperatures were assumed to be closer to the equilibrium conditions when heating curves are used. In our experience, a heating rate of 5 K/min enables spectra of sufficient quality for peak picking by hand with a reasonable experimental time, and the accuracy of the determined data is suitable for comparison with equilibrium conditions (CALPHAD Calculation). Nevertheless, experiments with different heating rates and an extrapolation of the 0 K/min heating rate would be best for determining the equilibrium phase transition temperatures.

B. Measurement and Analysis of Phase Composition

The compositions of the matrix and γ' -precipitate phases of EXP10-18 were measured by electron probe micro-analyzer (EPMA). For this purpose, the size of γ' -precipitates was deliberately increased to be several micrometers by a special heat treatment originally developed by Heckl *et al.*^[17]

To create extra-large γ' -precipitates, the fully heat-treated specimens were further heated to 1280 $^{\circ}$ C at a

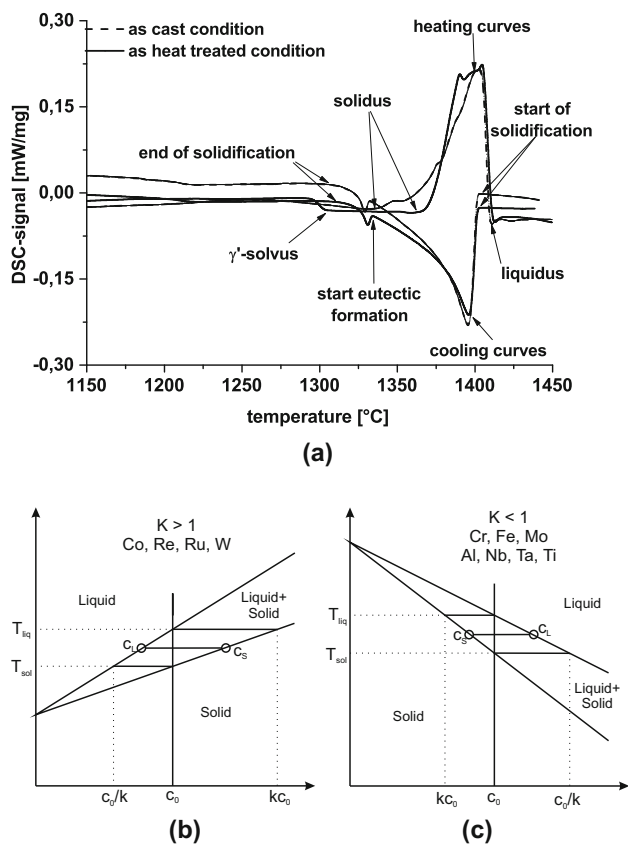


Fig. 1—(a) DSC results for as-cast (dashed lines) and heat-treated (solid lines) samples for a typical nickel-based superalloy, showing heating and cooling (ERBO/19^[19]). (b) and (c) Classification of alloying elements according to their influence on the solidus and liquidus temperature.

rate of 10 K/min, followed by annealing at a rate of 1 K/min up to 1290 $^{\circ}$ C, and holding at that temperature for 1 hour to achieve complete dissolution of the γ' -phase. A slow cool down to 1100 $^{\circ}$ C was then performed at approximately 20 K/h to create a small number of nucleating γ' -precipitates, which later grew

into large regions. The specimens were held for 12 hours at 1100 °C to allow growth of the precipitates. Afterwards, the temperature was slowly lowered for 8 hours to 700 °C to reduce the amount of tertiary γ' -precipitates formed. A coarsened microstructure with a precipitate size greater than 5 μm was formed and then investigated by EPMA (parameter set: electron beam diameter smaller 1 μm , spacing of 0.25 μm , and 100×100 points). The compositions of the matrix and precipitation phase were analyzed at five different spots for each phase. The specimens were clearly subjected to a wide range of temperatures during the coarsening anneal. For the purposes of comparison with calculated data, we assumed that experimental data represented the equilibrium phase compositions at a temperature of approximately 1000 °C.

C. Numerical Procedure

For every alloy composition, a property diagram (phase fraction vs temperature) was calculated by Thermo-Calc version 3.1 (Thermo-Calc, Solna, Sweden) with the databases TTNI8 (TermoTech, Surrey,

United Kingdom) and TCNI6 (Thermo-Calc, Stockholm, Sweden); MatCalc version 5.61 (MatCalc Engineering, Vienna, Austria) was also used with its database ME-NI (MatCalc Engineering, Vienna, Austria). Note that the MatCalc database was improved by consideration of the experimental data presented in this paper. From each property diagram, the transformation temperatures γ' -solvus, solidus, and liquidus were calculated. In addition, for the alloys from EXP10 to EXP18 the compositions of the matrix and γ' -phase at 1000 °C were extracted. All these values were compared with their corresponding experimental results.

III. RESULTS AND DISCUSSION

A. Influence of solid solution strengtheners Re, W, Mo, and Ru on transition temperatures in alloy group 1 and 2: i.e., EXP alloys with and without Ta

1. γ' -Solvus temperature

The effects of the solid solution strengtheners on the γ' -solvus are shown in Figure 2(a). The two different systems investigated included one with 2.5 at. pct Ta

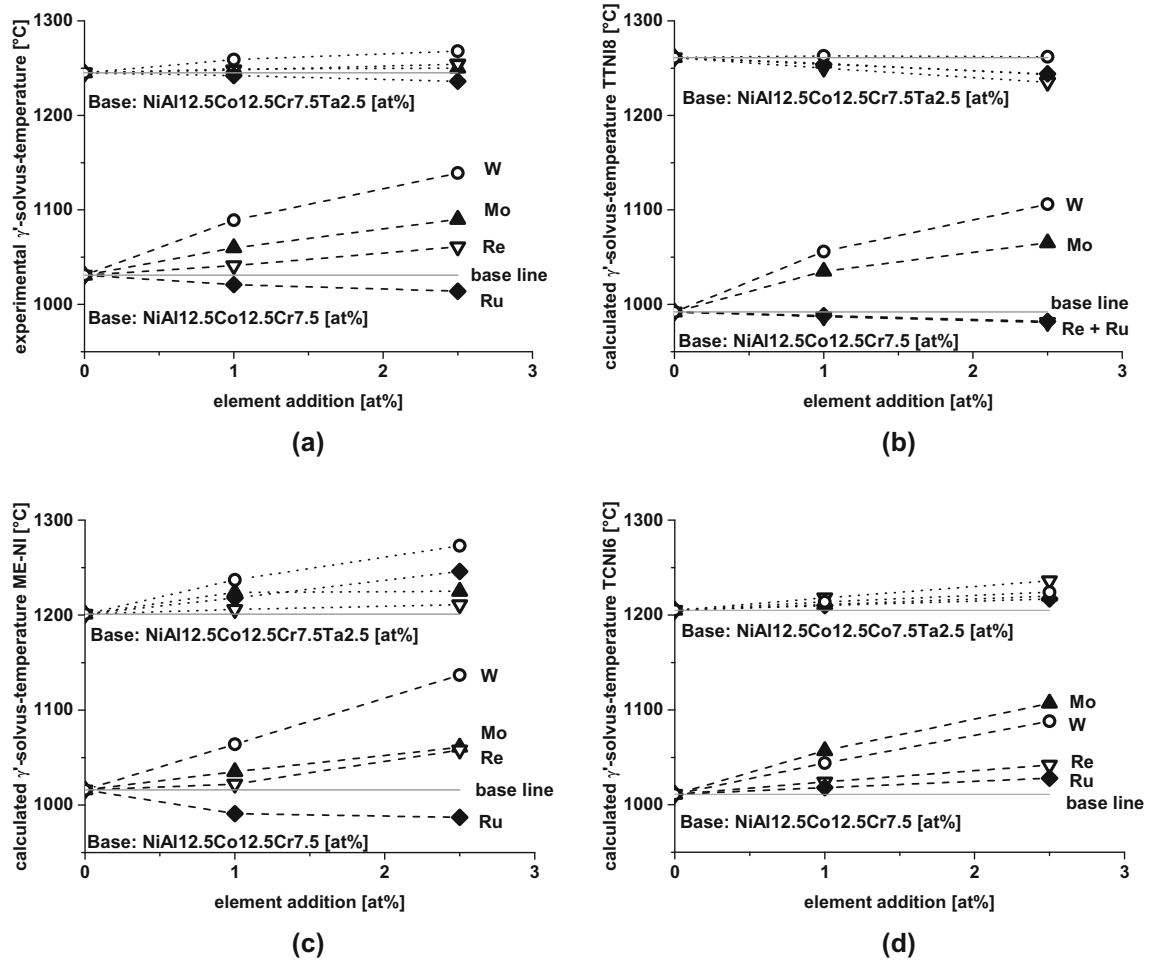


Fig. 2—Group 1 and 2: EXP alloys with and without Ta. Experimental and calculated results illustrating the effects of the solid solution strengthening elements on the γ' -solvus temperature. (a) Experimental results and results calculated with the databases (b) TTNI8, (c) ME-NI, and (d) TCNI6. If the two elements behaved in an identical way, the data points are labeled accordingly, (e.g., Re + Ru).

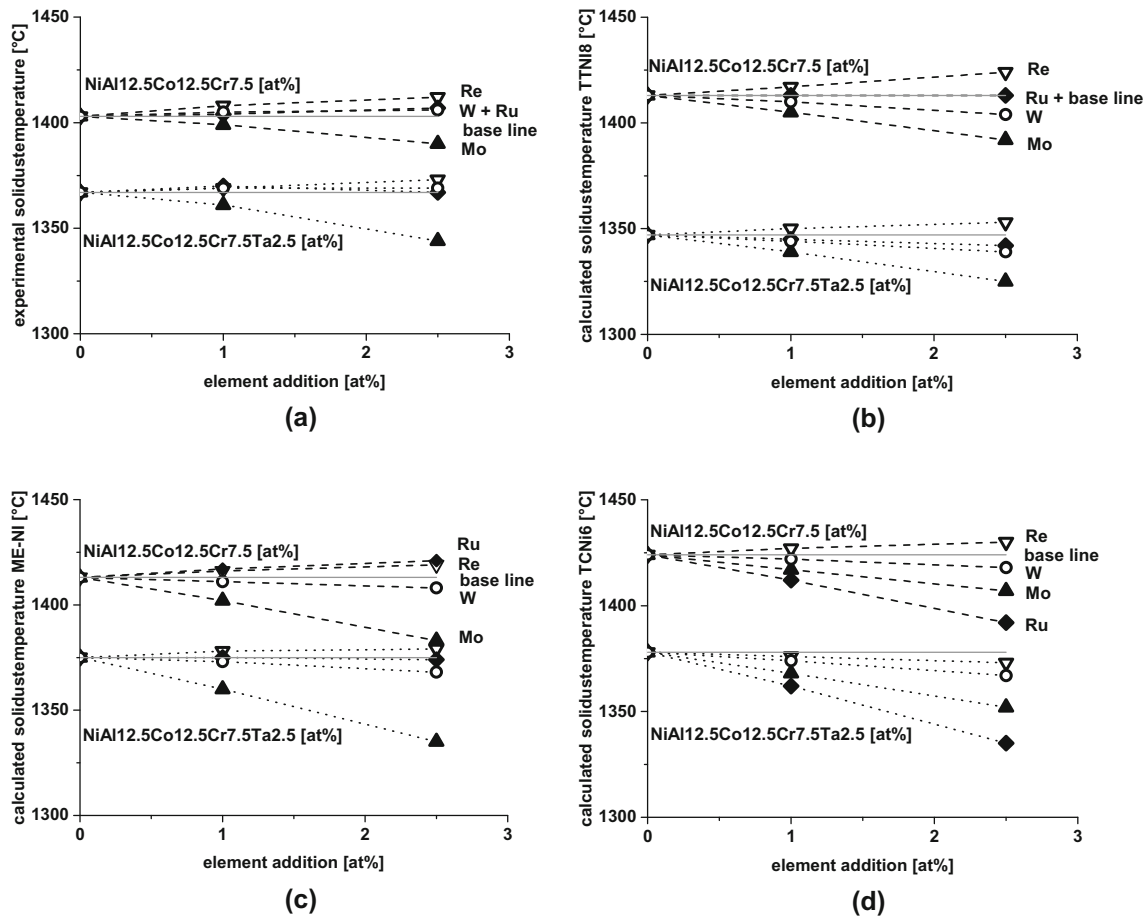


Fig. 3—Group 1 and 2: EXP alloys with and without Ta. Influence of the solid solution strengthening elements on the solidus temperatures. (a) Experimental results and results calculated with the databases (b) TTNi8, (c) ME-Ni, and (d) TCNi6. If two elements behaved identically, the data points are labeled accordingly (e.g., W + Ru).

and one without. The higher Ta content induced a higher γ' -volume fraction, as indicated by the difference between the γ' -solvus values for the Ta-free and Ta-containing systems (1031 °C vs 1245 °C). The strengtheners W, Mo, and Re increased the γ' -solvus temperature; however, Ru caused a slight decrease of the γ' -solvus temperature. This effect was more pronounced in the Ta-free alloy system than that in the Ta-containing system.

The addition of W showed the greatest effect on the γ' -solvus followed by Mo. The weakest effect was shown by Re. An increase of the γ' -solvus temperature is beneficial for precipitation strengthening because this increase suggests an increase in the γ' -phase fraction at the service temperature. It should be noted that this positive effect on precipitation strengthening is only effective when the precipitate size and the misfit size remain the same. Notably, the addition of W did show this beneficial effect on the γ' -solvus. The γ' -forming elements Ta, Ti, and Al are typically used to increase the γ' -solvus. However, this approach leads to a decrease of the solidus temperature, which hindered or even prevented the heat treatment. The addition of W contributed to both strengthening mechanisms, *i.e.*, the solid solution strengthening and precipitation

strengthening, without decreasing the solidus temperature. The effects of W on the solid solution strengthening have been investigated in detail by Fleischmann *et al.*^[20] On the basis of those results, W was ranked as the second best solid solution strengthener after Re, and was more effective than Mo.

Next, we compare the experimental findings (Figure 2(a)) with the thermodynamic calculations (Figures 2(b) through (d)). For a more comprehensive comparison, including all the experimental results of this paper, see the discussion below in Section III, and Figures 6, 7, and 8. The calculations based on the ME-Ni database gave the best overall accordance with the experimental results. The only deviation was that the influence of Ru in the Ta-containing alloy system was not accurately reproduced; however, this is unsurprising. The Me-Ni database was modified by its creators to incorporate the experimental findings of the present paper. This led to a clear improvement, expect with regard to the Ru influence in the Ta-containing alloy systems. The experimentally observed effects of Re in the Ta-free alloy system and the tendencies of Mo, Re, and W in the Ta-containing alloy system were also not accurately reproduced by calculations with the TTNi8 database. Nevertheless, the overall agreement for

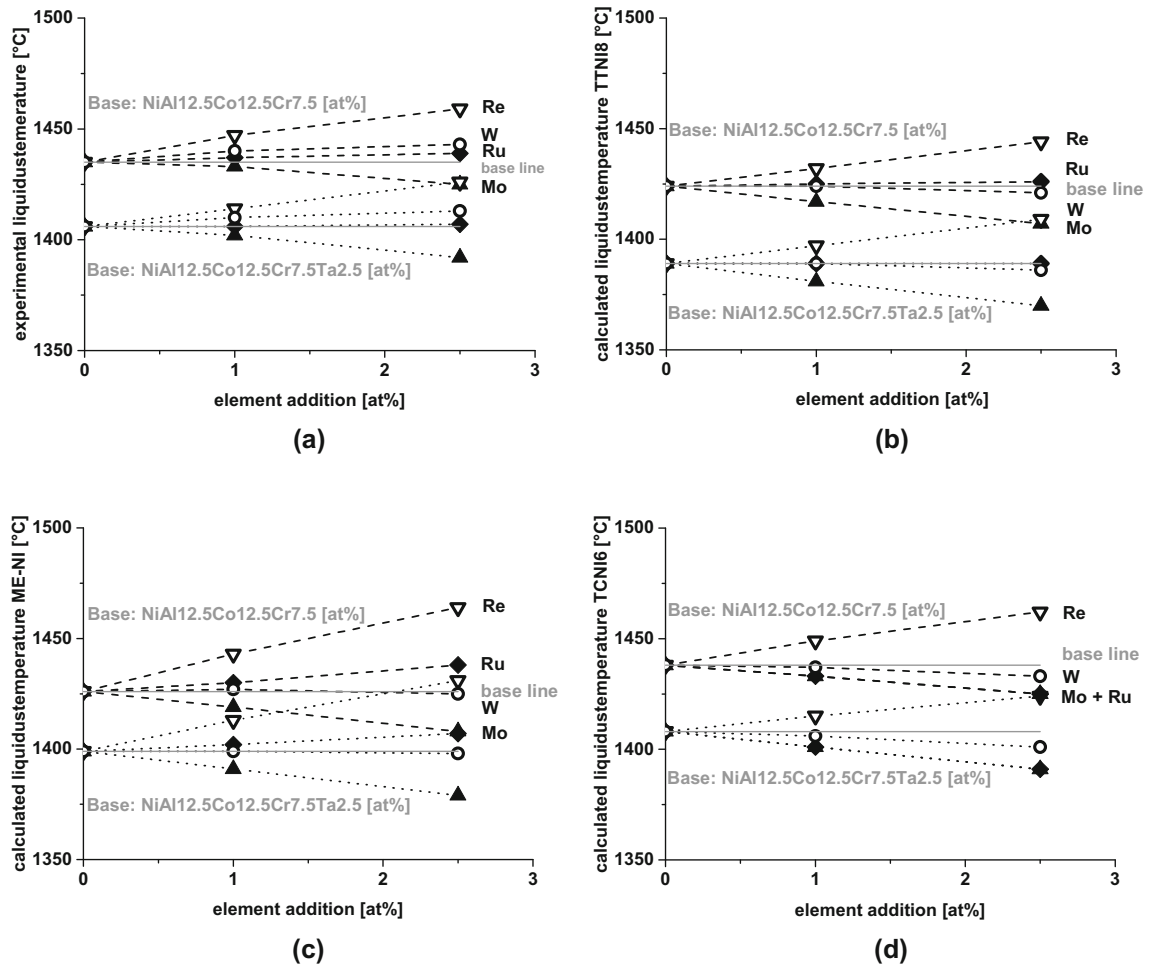


Fig. 4—Group 1 and 2: EXP alloys with and without Ta. Influence of solid solution strengthening elements on the liquidus temperatures. (a) Experimental results and results calculated with the databases (b) TTNi8, (c) ME-Ni, and (d) TCNi6. If two elements behaved identically, the data points are labeled accordingly (e.g., W + Ru).

TTNi8 was good. The TCNi6 database showed more notable deviations from the experimental results. The order in which the elements were predicted to increase the γ' -solvus temperature was incorrect and the overall tendency for Ru was not correctly predicted.

2. Solidus and liquidus temperature

Alloying elements can either increase or decrease the melting temperature. Figures 1(b) through (c) schematically illustrate these changes for binary systems. The solid solution strengtheners Re, Ru, and W typically increase the solidus and liquidus temperature; however, Mo lowers these transition points. Figures 3(a) and 4(a) present experimental results for the solidus and liquidus temperature, respectively, for the EXP alloy series studied in this paper. The effects on the solidus and liquidus are described above.

A comparison of the calculations from the different databases is shown in Figures 3(b) through (d) for the solidus and Figures 4(b) through (d) for the liquidus. The databases ME-Ni and TTNi8 showed good agreement between the experimental and calculated transition temperatures. Only the effects of W were not accurately described. The solidus and liquidus temperature should

increase rather than decrease as the element concentration increases. However, for TCNi6, two of the four overall tendencies were incorrect and the order in which the elements induced the increase was wrong. The main contribution to this error was attributed to the description of Ru. Instead of a slight increase of the solidus and liquidus temperature, TCNi6 predicted a strong decrease of both temperatures as the Ru content was increased. The TCNi6 database incorrectly predicted a decrease of the solidus temperatures compared with that of their base alloy for all elements added to the EXP alloys containing Ta. The influences of W on both transition temperatures were incorrectly determined, and similarly incorrect results were obtained from the use of TTNi8 and ME-Ni databases.

B. Influence of the Solid Solution Strengtheners Re and Ru on the Transition Temperatures of Alloy Group 3: ASTRA Alloys

The effects of Re and Ru in the Astra alloys (see Figure 5a) were similar to the results in the EXP alloy series, as presented above (Figures 2(a), 3(a), and 4(a)).

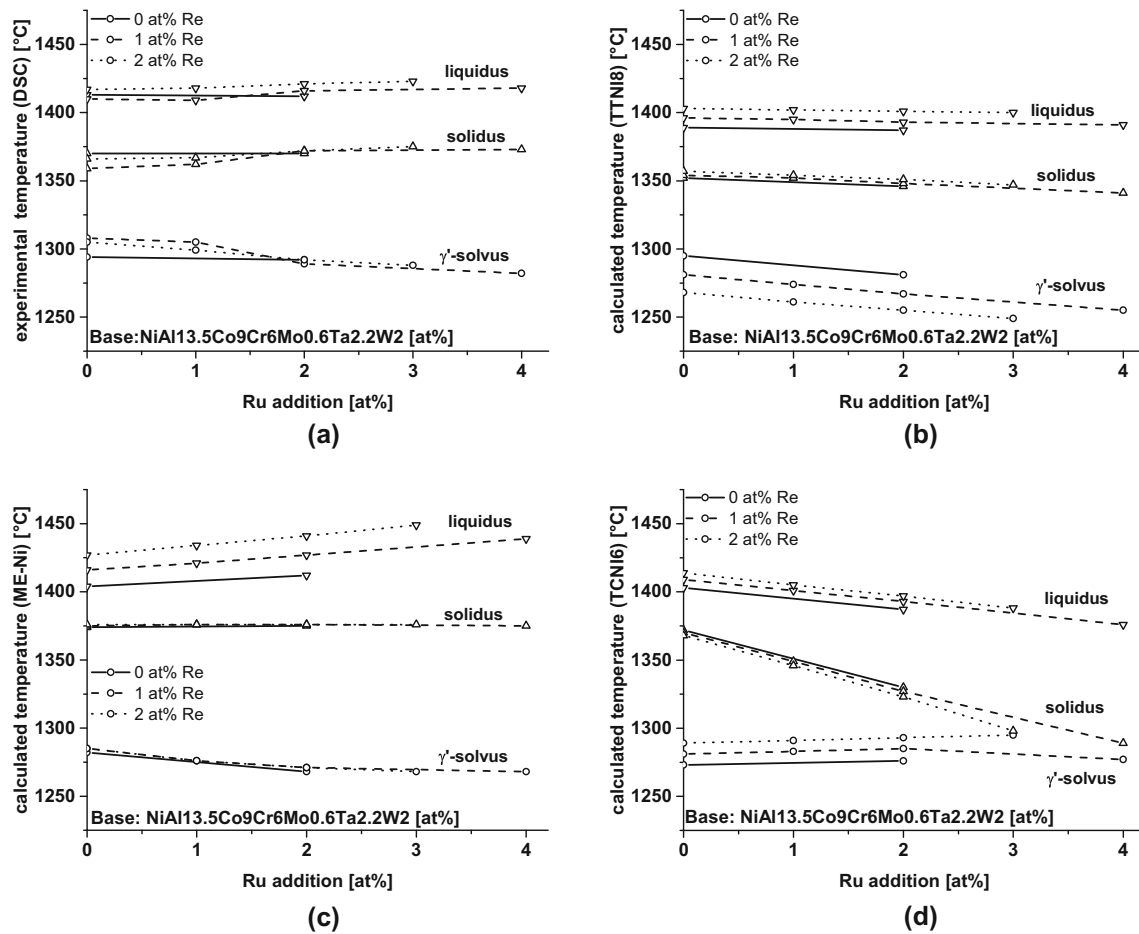


Fig. 5—Group 3: Astra alloys. Influence of Re and Ru on the transition temperatures. (a) Experimental results and results calculated with the databases (b) TTNi8, (c) ME-Ni, and (d) TCNi6.

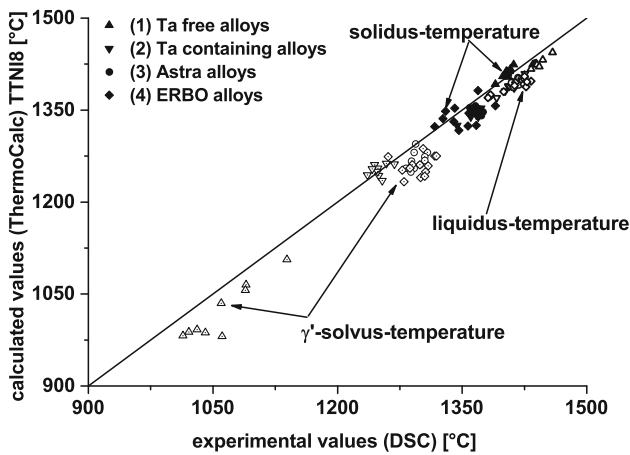


Fig. 6—Alloy groups 1 to 4. Comparison of experimental and calculated values based on the TTNi8 database.

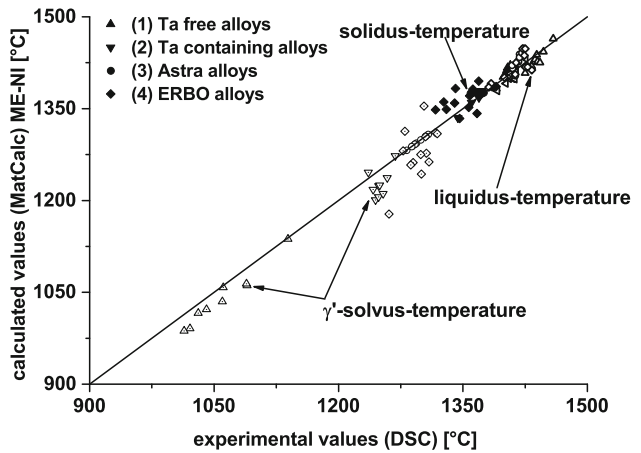


Fig. 7—Alloy groups 1 to 4. Comparison of experimental and calculated values based on the ME-Ni database.

Re increased and Ru decreased the γ' -solvus temperature (see Figure 5(a)). The decrease of the γ' -solvus temperature in the three different alloy groups is relevant because Ru has been shown to improve the phase stability of nickel-based superalloys, *i.e.*, Ru suppresses the formation of a detrimental TCP phase.^[12,14,16] Several

explanations have been given in literature to explain this behavior, such as reverse partitioning,^[12] changes of the surface energy,^[14] or increased solubility.^[13,15,16] The experimental findings in this study, of a reduction of the γ' -solvus and γ' -phase fraction, point to another explanation. It is likely that a reduction of the

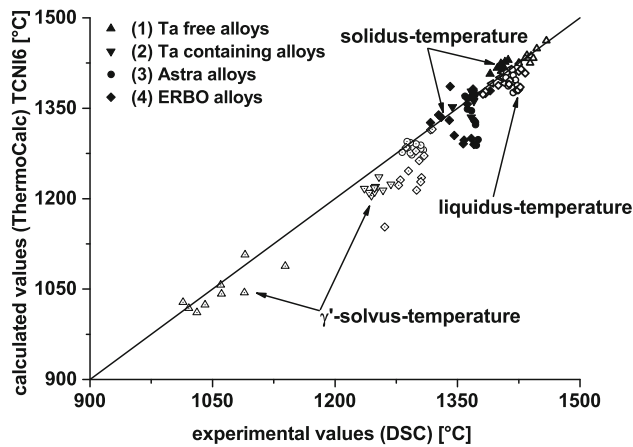


Fig. 8—Alloy groups 1 to 4. Comparison of experimental and calculated values based on the TCNI6 database.

concentration leads to less supersaturation of the TCP-forming elements in the matrix phase. This explanation was first proposed by Hobbs and Rae^[14] based on experimental γ' -phase fraction measurements for the alloy SRR300D with and without added Ru.

The solidus and liquidus temperatures were both increased by the addition of Re and Ru, and the effect of Re was more pronounced than that of Ru. In terms of the agreement between the experimental and calculated results, the two databases ME-NI and TTNi8 achieved the best match. The ME-NI database overestimated the effect of Re on the liquidus temperatures and TTNi8 calculations incorrectly suggested that the γ' -solvus temperature decreased as Re content increased. The TCNI6 database failed to correctly reproduce the influence of Ru on all three transition temperatures and therefore showed the worst overall performance for the investigated alloys.

C. Overall Comparison of Experimental and Calculated Phase Transition Temperatures—Alloy Groups 1 to 4

The data shown in Figures 2, 3, 4, and 5 are replotted in Figures 6, 7, and 8. Each figure represents values calculated for one particular database. The experimental findings for the alloy group 4 – ERBO alloys are also included.

For all databases, the deviations between the calculated and experimentally measured values were greater for the γ' -solvus than for the solidus and liquidus. The deviation of the γ' -solvus was greater for the TCNI6 database (root-mean-square error, RMSE = 38 K; $\Delta T_{\max} = 108$ K) than those for the other databases TTNi8 (RMSE = 35 K; $\Delta T_{\max} = 80$ K) and ME-Ni (RMSE = 27 K; $\Delta T_{\max} = 83$ K). Modeling of the precipitation and dissolution of a second phase in a multicomponent system is complex. All binary and ternary systems have to be adjusted and described as exactly as possible to achieve good results by extrapolation to high-order systems.

The RMSE analysis of the data scatter for the solidus (TTNi8: RMSE = 20 K, TCNI6: RMSE = 36 K, ME-NI: RMSE = 15 K) and liquidus temperatures

(TTNi8: RMSE = 21 K, TCNI6 = 20 K, ME-NI: RMSE = 14 K) showed that ME-NI gave the best performance, followed by TTNi8 and TCNI6.

The scatter of all the transformation temperatures was smallest for the results based on the ME-NI database (RMSE TTNi8: 26 K, RMSE TCNI6: 32 K, RMSE ME-NI: 19 K). However, the RMSE only takes into account the absolute difference between the calculated and experimentally measured values. A comparison of the results in Figures 6 through 8 shows that the TTNi8 database systematically overestimated the γ' -solvus and liquidus temperature for a given measurement for nearly all alloys. For the Ta-containing alloy group, the γ' -solvus temperature was systematically high owing to an overestimation of the temperature of the base alloy of this series. The ME-NI database also showed a number of overestimates, and there were even more for the TCNI6 database.

D. Phase Compositions and Partitioning Behavior in the Alloy Group 2: EXP Alloys with Ta

The left side of Figure 9 (Figures 9(a), (c), and (e)) shows the matrix and precipitate concentration of the elements Co, Cr, Al, and Ta in the alloys EXP10 to EXP18. The elements Co and Cr prefer to partition to the matrix phase, whereas Al and Ta partition to the precipitate phase.^[21] Owing to the adoption of our experimental results by the ME-NI database, this database showed the best overall agreement between the experimental and calculated values. Furthermore, the databases TTNi8 and TCNI6 were able to reproduce the general trends in the partitioning behavior; however, with these databases the deviation between experimental and calculated phase compositions was greater, particularly for TCNI6.

On the right side of Figure 9 (Figures 9(b), (d), and (f)), the matrix and precipitate concentration of the solid solution strengthening elements Mo, Re, Ru, and W in the alloys EXP10 to EXP18 are shown. In general, for all alloys, the strengthening elements were present in the matrix phase rather than the precipitate phase (except for W in the 1 at pct case). For Mo, Re, Ru, and W, the accordance of the calculated values and experimental measurements was not as good as for those for Co, Cr, Al, and Ta. The TTNi8 database failed to calculate the Re content in the γ' -phase and TCNI6 failed to predict the composition of the solid solution strengthening elements in the precipitation phase. The values for the matrix phase fitted well for all the databases; however, TCNI6 again showed the greatest deviation.

E. Critical Problems with the TCNI6 Database

Figure 10 shows property diagrams for ERBO/20 (based on EPM-102^[18]) and ERBO/21 (based on TMS-238^[2]). These are two highly alloyed nickel-based superalloys (see Table II). The calculations with the TTNi8 and ME-Ni databases showed typical behavior for such alloys, *i.e.*, a decrease of the γ' phase fraction with increasing temperature and TCP formation at low

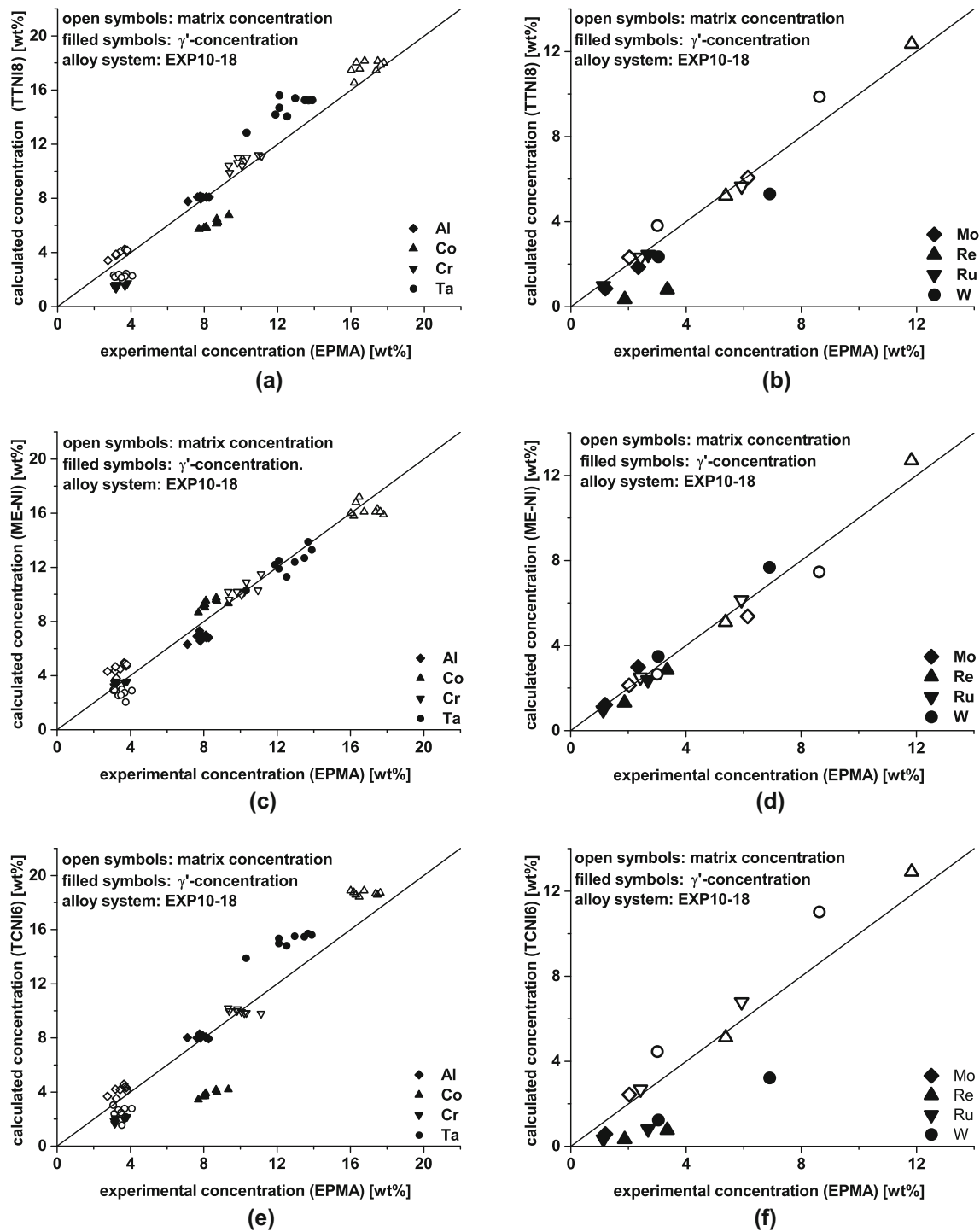


Fig. 9—Alloy group 2: EXP alloys with Ta. Composition of γ' -phase and γ -matrix. Comparison of experimental measurements and calculations for 1000 °C. The database used and the relevant elements are indicated in the figure. Figures (a), (c), and (e) show the comparison for Al, Co, Cr, and Ta and (b), (d), and (f) the results for solid solution strengtheners Mo, Re, Ru, and W.

temperatures owing to supersaturation of the matrix phase.

The calculation of the γ' -solvus temperature and the dependence of the γ' -phase fraction on temperature is a complex and failure-prone part of the phase calculation. This is particularly true for the TCNi6 database.

Moreover, for ERBO/20, the TCNi6 databases calculated a separation of the γ' -phase (FCC_A1#2 + FCC_A1#3, Figure 10(e)). The two γ' -phases differed in their chemical compositions but shared the same phase structure. However, this prediction was not supported by the experimental evidence. The erroneous

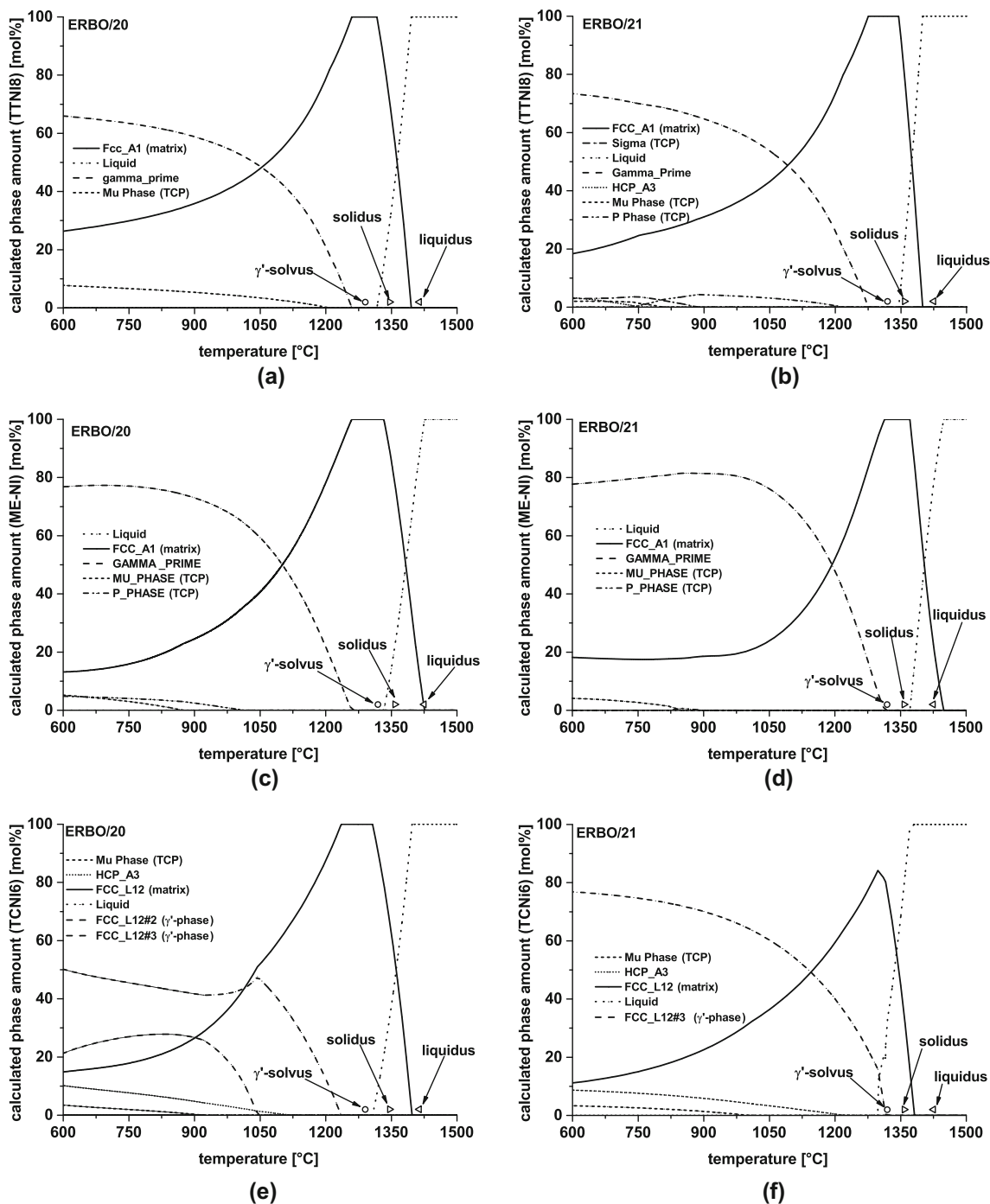


Fig. 10—Alloy group 4: ERBO alloys. Calculated property diagrams and experimentally determined transition temperatures for ERBO/20 (left) with the databases (a) TTNi8, (c) ME-NI, and (e) TCNi6. The ERBO/21 results (right) show calculations for ERBO/20 with the databases (b) TTNi8, (d) ME-NI, and (f) TCNi6.

phase separation behavior also influenced the proportion of the matrix phase and in turn the proportion of the TCP phase (μ -phase and HCP_A3, where HCP is not a TCP phase). Such phase separations were also found in predictions for Mo containing alloys EXP11 and EXP12. This phase separation was present in an earlier version of ME-NI for W- and Mo-rich alloys. This anomaly has been removed from ME-NI by

adjusting the description of the relevant binary and ternary systems.

Another major shortcoming of the TCNi6 database was pointed out earlier. The TCNi6 database does not correctly describe the effects of Ru on the transition temperatures. The incorrect calculation of the decrease in the solidus as Ru is added is misleading for alloy development (see Figure 10(f)).

The databases TTNI8 and the improved ME-Ni database show comparable and good results, that are useful for alloy development, although further improvements in the accuracy would be welcome. If the prediction of the γ' -solvus temperature is incorrect by more than 30 °C, the prediction of the γ' -phase fraction at the service temperature will also show a large discrepancy. The service temperature is close to the γ' -solvus. The good results achieved with the ME-NI database are unsurprising, because an improved version was used, which incorporated some of our own experimental results.

The calculation of the TCP phases was not the focus of the present paper and we emphasize that this issue remains a great challenge for the CALPHAD approach.^[16] Another similar challenge is the inclusion of elements that have not been widely used in superalloys in the past, such as Ge, and Ir. Such elements are of particular interest for future superalloy development.

IV. CONCLUSIONS

- W, Re, and Mo increased the γ' -solvus temperature. The addition of W contributed to both the solid solution strengthening of the matrix phase and to precipitation hardening. The contribution to the precipitation strengthening occurred through an increase of the precipitate volume fraction.
- The addition of Ru led to a decrease of the γ' -solvus temperature and γ' -volume fraction. By reduction of the γ' -phase fraction, supersaturation of the matrix phase with respect to the TCP phase was reduced, which might explain the improvement of the phase stability by Ru addition.
- The TTNI8 database and the improved ME-NI database showed good agreement with experimental data, in particular when the accuracy of the measurements was taken into account. Predictions with the TCNI6 database showed much greater deviation for this materials system.

ACKNOWLEDGMENTS

The authors acknowledge funding from the German Science Foundation (DFG) in the framework of the Collaborative Research Center/Transregio 103 (Projects B1, C7, and Z01) as well as MTU Aero Engines AG and the German Federal Ministry of Economic Affairs and Energy within the Aeronautical Research Programme V/1. Our institute colleagues Sabine Michel and Peter Randelzhofer are gratefully thanked for EPMA measurements and DSC measurements. Similarly, Prof. Ernst Kozeschnik from the Institute of Material Science and Technology at TU Vienna is

gratefully thanked for providing the MatCalc software and database in the framework of Aeronautical Research Programme V/1. We thank Andrew Jackson, PhD, from Edanz Group (www.edanzediting.com/ac) for editing a draft of this manuscript.

OPEN ACCESS

This article is distributed under the terms of the Creative Commons Attribution 4.0 International License (<http://creativecommons.org/licenses/by/4.0/>), which permits unrestricted use, distribution, and reproduction in any medium, provided you give appropriate credit to the original author(s) and the source, provide a link to the Creative Commons license, and indicate if changes were made.

REFERENCES

1. R.C. Reed, J.J. Moverare, A. Sato, F. Karlsson, M. Hasselqvist: *TMS2012*, 2012, pp. 197–204.
2. K. Kawagishi, A.C. Yeh, T. Yokokawa, T. Kabayashi, Y. Koizumi, H. Harada: *TMS2012*, 2012, pp. 189–95.
3. Y. Shmotin, A. Logunov, D. Danilov, I. Leshchenko: 8th Pacific Rim International Congress on Advanced Materials and Processing, *TMS2013*, 2013, pp. 327–36.
4. R. Rettig, N.C. Ritter, H.E. Helmer, S. Neumeier, and R.F. Singer: *Modell. Simul. Mater. Sci. Eng.*, 2013, vol. 23, pp. 1–24.
5. N. Saunders and A.P. Miodownik: *Calculation of Phase Diagrams*, Pergamon Press. Inc., Oxford, 1996.
6. U.R. Kattner: *JOM*, 1997, vol. 12, pp. 14–19.
7. Y.A. Chang, S. Chen, F. Zhang, X. Yan, F. Xie, R. Schmid-Fetzer, and W.A. Oates: *Prog. Mater. Sci.*, 2004, vol. 49, pp. 313–45.
8. H. Lukas, S.G. Fries, B. Sundman: Cambridge University Press., 2007.
9. C.M.F. Rae and R.C. Reed: *Acta Mater.*, 2007, vol. 55, pp. 1067–81.
10. F.A. Schweizer, D.N. Duhl: US-Patent No. 4; 222, 794; 1980.
11. A.F. Giamei and D.L. Anton: *Metall. Trans. A*, 1985, vol. 16A, pp. 1985–97.
12. K.S. O'Hara, W.S. Walston, E.W. Ross, R. Darolia: US-Patent No. 5, 482, 789; 1996.
13. A. Sato, H. Harada, T. Yokokawa, T. Murakumo, Y. Koizumi, T. Kobayashi, and H. Imai: *Scripta Mater.*, 2006, vol. 54, pp. 1679–84.
14. R.A. Hobbs, L. Zhang, C.M.F. Rae, and S. Tin: *Metall. Mater. Trans. A*, 2008, vol. 39A, pp. 1014–25.
15. A. Heckl, S. Neumeier, S. Cenanovic, M. Göken, and R.F. Singer: *Acta Mater.*, 2011, vol. 59, pp. 6563–73.
16. K. Matuszewski, R. Rettig, H. Matysiak, Z. Peng, I. Povstugar, P. Choi, J. Müller, D. Raabe, E. Spiecker, K.J. Kurzydowski, and R.F. Singer: *Acta Mater.*, 2015, vol. 95, pp. 274–83.
17. A. Heckl, S. Neumeier, M. Göken, and R.F. Singer: *Mater. Sci. Engine. A*, 2011, vol. 528, pp. 3435–44.
18. S. Walston, A. Cetel, R. MacKay, K.O' Hara, D. Duhl, R. Dreshfield: *TMS2004*, 2004, pp. 15–24.
19. N.C. Ritter, E. Schesler, A. Müller, R. Rettig, C. Körner, and R.F. Singer: *Adv. Engine. Mater.*, 2017, <https://doi.org/10.1002/adem.201700150>.
20. E. Fleischmann, M.K. Miller, E. Affeldt, and U. Glatzel: *Acta Mater.*, 2015, vol. 87, pp. 350–6.
21. F. Pyczak, B. Devrient, F.C. Neuner, and H. Mughrabi: *Acta Mater.*, 2005, vol. 53, pp. 3879–91.